COMPUTING THE REEB GRAPH FOR TRIANGLE MESHES WITH ACTIVE CONTOURS

Laura Brandolini and Marco Piastra
Computer Vision and Multimedia Lab, Università degli Studi di Pavia, via Ferrata 1, 27100 Pavia, Italy

Keywords: Reeb graph, Active contours, Triangle mesh, Segmentation.

Abstract: This paper illustrates a novel method to compute the Reeb graph for triangle meshes. The algorithm is based on the definition of discrete, active contours as counterparts of continuous level lines. Active contours are made up of edges and vertices with multiple presence and implicitly maintain a faithful representation of the level lines, even in case of coarse meshes with higher genus. This approach gives a great advantage in the identification of the nodes in the Reeb graph and also improves the overall efficiency of the algorithm in that at each step only the information local to the contours and their immediate neighborhood needs to be processed. The validation of functional integrity for the algorithm has been carried out experimentally, with real-world data, without mesh pre-processing.

1 INTRODUCTION

Reeb graphs are compact shape descriptors that play a fundamental role in different fields of computer graphics: shape matching and encoding (Sebastian et al., 2002; Sundar et al., 2003), mesh deformation (Tierny et al., 2006; Schaefer and Yuksel, 2007), 3D search (Hilaga et al., 2001), mesh compression (Biasotti et al., 2000), medical imaging and several other fields. Reeb graphs enclose important shape properties like connectivity, length, width, direction and genus in a faithful fashion.

This paper illustrates a new robust method for constructing Reeb graphs for 2-manifold, triangle meshes using a predefined Morse function. In the literature there are other methods for Reeb graphs extraction, as it will be described in Section 3. In Section 4 we propose an approach in which the Reeb graph is constructed incrementally by evolving discrete, active contours over the mesh, starting from relevant minima of the Morse function. A key aspect in the active contours proposed is that both vertices and edges could have a multiple presence and this allows a faithful representation of the level lines of the Morse function even when these lines are too close to each other with respect to mesh sampling.

Experimental evidence, illustrated in Section 5, shows that this algorithm is effective with real-world data, without the need of pre-processing, and therefore suitable for practical applications.

2 THEORETICAL PRELUDE

Morse theory (Milnor, 1963) is a classical mathematical approach that has found many applications in the field of *computational topology*. The Morse function f is a real-valued function defined on a compact smooth manifold M (Biasotti et al., 2008). A point x of M where all the partial derivatives of f are zero is a *critical point*. A critical point x is *non-degenerate* if the matrix of second order partial derivatives (*Hessian*) of f at x is non-singular. A non-degenerate critical point can only be a maximum, a minimum or a saddle, while other points are called *regular*. We can then define a Morse function as a smooth function f defined on M that has no degenerate critical points. The function f is frequently required to be *simple*, i.e. $f(x) \neq f(y)$ for any pair x and y of distinct critical points.

Reeb graphs have been defined by George Reeb in 1946 (Reeb, 1946). Given a compact, smooth manifold M and a Morse function f defined on it, the Reeb graph "is the quotient space defined by the equivalence relation that identifies the points belonging to the same connected component of the level-set of f". Each point in a Reeb graph corresponds to a connected component of a level set of the Morse function f. In particular, each point of the arcs in the graph corresponds to a regular value of f, whereas each node corresponds to a critical value of f. Reeb graphs are compact shape descriptors which convey topological

Brandolini L. and Piastra M. (2012).
COMPUTING THE REEB GRAPH FOR TRIANGLE MESHES WITH ACTIVE CONTOURS.
In *Proceedings of the 1st International Conference on Pattern Recognition Applications and Methods*, pages 80-89
DOI: 10.5220/0003745500800089

information about the shape of the manifold M. In particular for orientable, closed 2-manifolds the number of loops in the Reeb graph corresponds to the *genus* of the manifold (Cole-McLaughlin et al., 2003) and this property does not depend on the choice of the Morse function f.

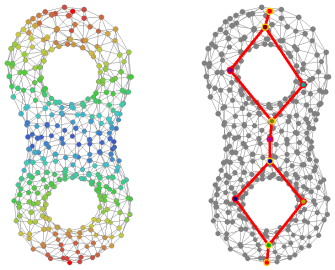

(a) (b)

Figure 1: A discrete Morse function with *two* minima (see text) (a); the corresponding discrete Reeb graph (in red), where the nodes are emphasized in orange (b).

3 RELATED WORK

Reeb graphs have been extensively applied in recent years in different fields of computer science, thus a complete exploration of all the contributions about this matter is beyond the scope of this paper. Detailed works on the subject of Reeb graphs for shape analysis can be found in (Biasotti et al., 2008). The introduction of Reeb graphs in computer graphics is due to (Shinagawa et al., 1991) and the first algorithm to automatically compute Reeb graphs is described in (Shinagawa and Kunii, 1991). This algorithm automatically constructs the Reeb graph of a 2D manifold surface embedded in 3D using surface contours, a weight function and an a priori knowledge of the number of holes of the object. In their work (Lazarus and Verroust, 1999) describe an algorithm that constructs level-set diagrams for 0-genus polyhedrons using geodesic distance from a source point. (Tierny et al., 2006) propose a smart approach based on a good choice of the Morse function f, taking feature points as the origin of function f, but the strategy adopted for evolving contours leads to critical contour configurations, especially in case of coarse, real-world meshes. (Pascucci et al., 2007) propose an on-line algorithm for Reeb graphs construction and test its performance with different Morse functions. Their algorithm has an iterative approach that requires taking into account all the simplicial elements of the mesh (vertices, edges and triangles) during the computation: at each step, a new simplicial element is considered and the Reeb graph is incrementally updated, until all simplicial elements have been considered. (Shapira et al., 2008) propose an algorithm for mesh decomposition and skeletonization using a shape diameter function (SDF), i.e. a scalar function defined on mesh faces. This technique is pose-invariant in general, but there are positions for which smoothing and filtering are necessary. In (Edelsbrunner et al., 2008) an algorithm is presented to calculate the Reeb graph of a time-varying continuous function defined in the tridimensional space. They give also a classification of the combinatorial changes in the evolution of the Reeb graph of a time-varying Morse function. (Doraiswamy and Natarajan, 2009) propose an approach for computing Reeb graphs with the use of dynamic graphs, but also in this case a global sorting step is needed to start the computation. A work by (Berretti et al., 2009) proposes a 3D mesh segmentation using Reeb graphs. As in (Hilaga et al., 2001) this work uses AGD (*average geodesic distance*) calculated from a small set of evenly-spaced vertices (*base vertices*) and this choice leads to inaccurate results with certain type of meshes. (Patane et al., 2009) propose an approach for building the Reeb graph of a mesh using critical points and their isocontours, which is particularly suited for large meshes with small genus and really smooth functions (with a small number of critical points), but is not suited for coarse meshes with higher genus.

4 THE ALGORITHM

A key aspect in the algorithm proposed are *active contours*, namely ensembles of vertices and edges with possible *multiple presence*, that represent the level lines of the Morse function.

On a 2-manifold and away from critical points, each level line is a 1-manifold, possibly with more than one connected component, which become either a point or a self-intersecting line when critical points are met. The representation of each connected component by an active contour relies on the multiple presence of vertices and edges in order to preserve such 1-manifoldness for all regular values. In fact, when the mesh is coarse, the immediate discrete representation would not be a 1-manifold (see for instance Figures 3(a) and 4(a)). In addition, as we will see, the multiple presence of vertices in active contours simplifies the detection of saddles, i.e. where active contours either *split* or *merge*. Indeed, as it will be seen later on, in our algorithm split and merge events can only occur with vertices with presence greater than 1 in either the same contour (split) or in two different contours (merge). The mesh segmentation is generated as a by-product, by associating

to each active contour a segment, which is closed and created anew whenever a critical point is met.

The overall algorithm can be summarised as follows:

- compute the values of the Morse function for each vertex;
- identify the prominent points of the mesh - i.e. *feature points* - each corresponding to relevant minima in the Morse function;
- initialize an active contour at each feature point;
- evolve incrementally all the active contours in the direction of increasing values of the Morse function;
- perform either split or merge operations each time a critical point is detected (see Figure 1(b));
- terminate the execution when all active contours have reached a maximum.

4.1 Which Morse Function

We opted for the same Morse function adopted in (Tierny et al., 2006). This particular function is bound to intrinsic shape properties, as described in the above paper, and therefore is both robust in front of variation in mesh sampling and invariant to mesh rotation and deformation.

The Morse function in point is based on the concept of *geodesic distance* on a mesh (Novotni et al., 2002), meant as the length of the shortest path connecting each two vertices. A derived concept is that of *diameter vertices*: i.e. a pair of vertices that are at the maximum geodesic distance on the mesh. A pair of diameter vertices can be found with a recursive algorithm, as illustrated in (Lazarus and Verroust, 1999).

The Morse function is computed through the following steps:

- find the two diameter vertices (see above) and calculate the two distance functions from these points with the Dijkstra algorithm (Dijkstra, 1959);
- find the local maxima and minima of the two distance functions, i.e. the local extrema;
- identify the *feature points* (*FP*) by merging local extrema with some tolerance (see below);
- calculate the Morse function, defined as the geodesic distance between each vertex and the closest *FP*, with the Dijkstra algorithm.

4.1.1 Find Diameter Vertices and Mesh Maximum Distance

The algorithm randomly chooses a *starting vertex* in the mesh and sets it as the *currentVertex*. Then it calculates the distance map, with the Dijkstra algorithm, and finds the most distant vertex. The latter is selected as the next *currentVertex* and the algorithm repeats itself until *currentVertex* and its most distant vertex in 2 consecutive loops coincide. We call these two vertices *diameter vertices V1* and *V2* respectively. It is worth highlighting that this method is fairly robust in practise, in that the resulting diameter vertices depend only weakly on the choice of the starting vertex.

The two diameter vertices define *two* distance functions:

- δ_1: the distance from diameter vertex *V1*
- δ_2: the distance from diameter vertex *V2*

The distance between the couple of points *V1* and *V2* is defined as the *maxDistance* and will be used to normalize all distances in the mesh. In this way the value of the parameters in the algorithm will be independent from the actual size of the mesh.

4.1.2 Identification of Feature Points

Feature points (*FP*) are usually defined in the literature (Mortara and Patane, 2002) (Katz et al., 2005) (Tierny et al., 2006) as the vertices in the mesh that are furthest away from every other mesh vertex. Typically they are located on mesh prominent components.

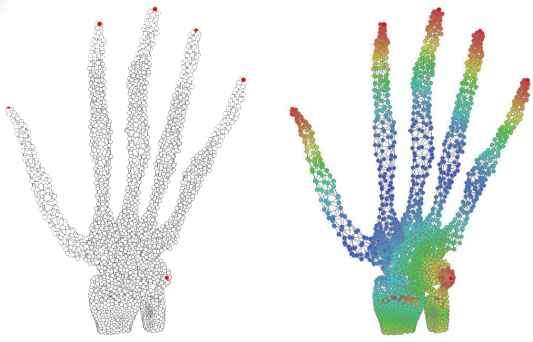

(a) (b)

Figure 2: Feature points (in red) (a) and the resulting distance function δ (b).

Following (Tierny et al., 2006) we identify feature points by merging the *local extrema* of the two distance functions δ_1 and δ_2. Local minima and local maxima from either functions that are not farther away than a certain predefined tolerance value reinforce each other and are merged in a common feature

point, whereas isolated extrema are simply discarded (see Figure 2(a)).

4.1.3 The Morse Function

The Morse function of our choice is defined as the normalized geodesic distance between each vertex and the closest feature point (see Figure 2(b)). In agreement with (Tierny et al., 2006) we also perform a post-processing step in order to ensure that no two vertices have the same value of the Morse function.

4.2 Computing the Reeb Graph

4.2.1 Discrete Contours as Multisets

In a theoretical framework, a Morse function f defined on a continuous and smooth surface implicitly defines level lines that join all the points at the same value of f. In our context, the Morse function f is defined only at mesh vertices and, per choice, the discrete representation of level lines is made only of mesh edges and vertices. Besides the loss of precision, which is easily addressable, a critical problem is that the discrete representation of a level line might no longer be 1-manifold. As a matter of fact, this problems occurs frequently on coarse meshes (see Figure 3(a)-4(a)). In order to solve this we borrow an idea from (Edelsbrunner et al., 2003) in that we introduce *multiple presence* of both edges and vertices in the discrete representation of level lines.

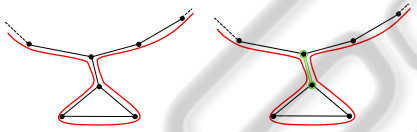

(a) (b)

Figure 3: The continuous level line - in red - is a 1-manifold, while its discrete representation is not (a). In the representation with multiple presence (double vertices and edges - in green) the 1-manifoldness of the level line is implicitly maintained (b).

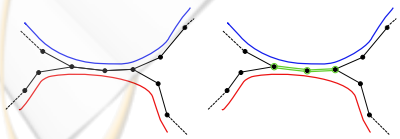

(a) (b)

Figure 4: In this case the discrete representation with multiple presence maintains the 1-manifoldness of each corresponding level lines.

In other words, what we will call in the following an *active contour* γ, is made of two *multisets* (Knuth, 1998) of vertices and edges respectively.

As shown in Figures 3(b) and 4(b), *active contours* maintain the representation of discrete contours faithful with respect to the continuous level lines.

Due to obvious topological reasons, in a triangle mesh, the vertices with multiple presence can only exist in an active contour in a fixed number of patterns, as represented in Figures 5,6,7. These figures describe all the possible, base configurations of a segment of the discrete contour, with multiple presence of vertices up to 3 and multiple presence of edges up to 2.

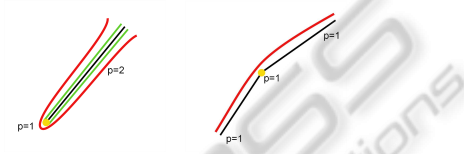

(a) (b)

Figure 5: The catalog of all possible configurations of one vertex with presence 1 in a contour.

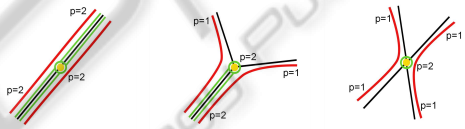

(a) (b) (c)

Figure 6: The catalog of all possible configurations of one vertex with presence 2 in a contour.

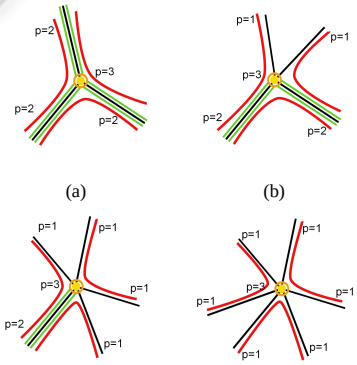

(a) (b)

(c) (d)

Figure 7: The catalog of all possible configurations of one vertex with presence 3 in a contour.

In our experience, with meshes up to genus 22, we found no evidence of presences higher than the ones above. We suspect the existence of a theoretical limit about those values, given suitable quality conditions for the mesh. In any case multiple presences with greater values could be accommodated by modifying the algorithm accordingly.

The multiple presence of vertices and edges results in a great advantage in detecting split or merge

events. Indeed, as it will be shown in 4.2.3, split and merge events can only occur at vertices with presence greater than 1.

4.2.2 The Main Algorithm

Initially all feature points become an active contour and active contours evolve in a way that is shown in detail in Algorithm 4.1.

There are two crucial events in contour evolution:
Split: when a single contour separates in two different, disconnected contours.
Merge: when two contours melt in one unique, connected contour.

Active contours γ sweep the mesh, following the direction of ascending values of the Morse function. γ is made of two multisets:

- V: active contours vertices
- E: active contours edges

The ensemble of segments σ is extracted during the evolution of active contours. Each segment σ is made of:

- γ: the active contour of the segment (used in read-write for segmentation)
- V: the visited vertices of the segment (used as write-only repository during segmentation)

The set that collects all active segments is called Σ. Once an event occurs (either merge or split) the active segments involved are *closed* and stored in Σ_c, the set of segments that have already been closed.

4.2.3 Evolution of Active Contours

In the main loop, at each step, a candidate vertex v_c is selected as the one with the lowest value of the Morse function in all active contours.

$$\sigma = \textbf{\textit{nearest}}(\Sigma), v_c = \textbf{\textit{nearest}}(\sigma.\gamma) \qquad (1)$$

The algorithm first checks the presence of the candidate vertex v_c in the active contour, as a presence greater than one would reveal a split event, then it checks for the presence of v_c in other contours, in order to detect a merge event. Then the contour is updated locally.

This operation is described in detail in Algorithm 4.2 and illustrated in Figure 8. In the description that follows we use the concepts of *star* and *link* of a vertex in a *simplicial complex* - see for instance (Edelsbrunner, 2001) for details. In the basic step of contour evolution, the *star* of v_c on the *contour* (see Figure 8(a)) is replaced by a subset of the *link* of v_c on the *mesh* (see Figure 8(b)), in the direction of advancement. More precisely, the replacing subset of the link of v_c on the mesh, which we call the $link^+$, has a fairly subtle definition. The link of v_c is divided by the vertices that also belong to the active contour into connected subsets. By definition, the $link^+$ is obtained by subtracting from the link of v_c all the connected components that contain at least one vertex having a value of the Morse function which is lower than the one on v_c.

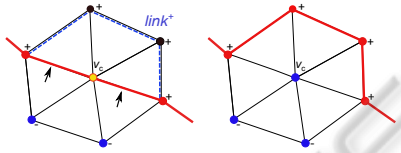

(a) (b)

Figure 8: Local update of the contour: the star of v_c on the contour (a) is replaced by the $link^+$, i.e. a subset of the link of v_c on the mesh (b).

4.2.4 Finding Connected Components

If each active contour was composed only of vertices and edges with a single presence, the separation of connected subsets would be straightforward.

The multiple presence of both edges and vertices makes the problem more complex, as shown in Figure 9. In particular, when visiting the double branch (i.e. the green segment containing double presence edges and vertices) from one side, it is crucial to exit from "the right side" of the contour, i.e. without crossing over. In our method it is possible to discriminate the direction to be kept by inspecting the values of the Morse function in the local neighborhoods. In Figure 9(a) we identify the subset of the link (in blue) of an entrance vertex a, as the one being delimited by two contour vertices and containing the vertex that is the intersection between the link of the vertex a and the subsequent vertex b, with a lower value of the Morse function and not belonging to the active contour. This lets us determine by intersection the right subset (in violet) of the link of the subsequent vertex b. The procedure can be repeated until the entire double branch has been visited. Figure 9(b) shows that the visiting procedure exits from the right side in that it properly selects vertex e over vertex f as the exit vertex.

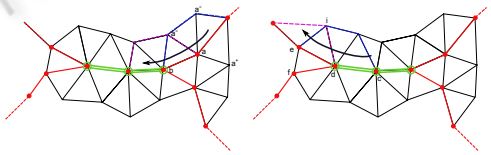

(a) (b)

Figure 9: Finding connected components in an active contour: how to walk a double branch.

Algorithm 4.1: SEGMENTATION(FPs)

main
INITIALIZE(FPs)
while $not(\Sigma = \emptyset)$
$\sigma = \textbf{\textit{nearest}}(\Sigma), v_c = \textbf{\textit{nearest}}(\sigma.\gamma)$
if $\textbf{\textit{presence}}(v_c, \sigma.\gamma) > 1$
then SPLIT(v_c, σ)
else **if** $\exists \sigma_1 : v_c \in \sigma_1.\gamma$
then MERGE(σ, σ_1)
else ADVANCECONTOUR(v_c, σ)

procedure INITIALIZE(FPs)
$\Sigma, \Sigma_c = \{\emptyset\}$
for each $fp \in FPs$
do $\sigma = \textbf{\textit{new}}(\sigma)$; $\sigma.\gamma.V = \sigma.\gamma.V \cup \{fp\}$; $\sigma.V = \sigma.V \cup \{fp\}$; $\Sigma = \Sigma \cup \sigma$

procedure ADVANCECONTOUR(v_c, σ)
$linkPlus =$ FINDLINKPLUS($v_c, \sigma.\gamma$)
$\sigma_{updated} = \textbf{\textit{updateContour}}(\sigma, v_c, linkPlus)$
$\textbf{\textit{removeFolds}}(\sigma_{updated}.\gamma)$
$\Sigma = \Sigma \cup \sigma_{updated} - \sigma$

procedure MERGE(σ_1, σ_2)
$\sigma_{merged}.\gamma.V = \sigma_1.\gamma.V \cup \sigma_2.\gamma.V$
$\sigma_{merged}.\gamma.E = \sigma_1.\gamma.E \cup \sigma_2.\gamma.E$
$linkPlus =$ FINDLINKPLUS($v_c, \sigma_{merged}.\gamma$)
$\sigma_{updated} = \textbf{\textit{updateContour}}(\sigma_{merged}, v_c, linkPlus)$
$\textbf{\textit{removeFolds}}(\sigma_{updated}.\gamma)$
$\textbf{\textit{setAdjacence}}(\sigma_1, \sigma_{updated})$
$\textbf{\textit{setAdjacence}}(\sigma_2, \sigma_{updated})$
$\Sigma_c = \Sigma_c \cup \{\sigma_1, \sigma_2\}$
$\Sigma = \Sigma \cup \sigma_{updated} - \{\sigma_1, \sigma_2\}$
$\Gamma = \textbf{\textit{connectedComponents}}(\sigma_{updated}.\gamma)$
if $\Gamma.size > 1$
then $\sigma_a = \textbf{\textit{splitSegment}}(\sigma_{updated}, \Gamma[0])$; $\sigma_b = \textbf{\textit{splitSegment}}(\sigma_{updated}, \Gamma[1])$; $\textbf{\textit{setAdjacence}}(\sigma_a, \sigma_{updated})$; $\textbf{\textit{setAdjacence}}(\sigma_b, \sigma_{updated})$; $\Sigma = \Sigma \cup \{\sigma_a, \sigma_b\} - \sigma_{updated}$; $\Sigma_c = \Sigma_c \cup \sigma_{updated}$

procedure SPLIT(v_c, σ)
$linkPlus =$ FINDLINKPLUS($v_c, \sigma.\gamma$)
$\sigma_{updated} = \textbf{\textit{updateContour}}(\sigma, v_c, linkPlus)$
$\textbf{\textit{removeFolds}}(\sigma_{updated}.\gamma)$
$\Gamma = \textbf{\textit{connectedComponents}}(\sigma_{updated}.\gamma)$
if $\Gamma.size > 1$
then $\sigma_1 = \textbf{\textit{splitSegment}}(\sigma, \Gamma[0])$; $\sigma_2 = \textbf{\textit{splitSegment}}(\sigma, \Gamma[1])$; $\textbf{\textit{setAdjacence}}(\sigma_1, \sigma)$; $\textbf{\textit{setAdjacence}}(\sigma_2, \sigma)$; $\Sigma_c = \Sigma_c \cup \{\sigma\}$; $\Sigma = \Sigma \cup \{\sigma_1, \sigma_2\} - \sigma$
else $\Sigma = \Sigma \cup \sigma_{updated} - \sigma$

Algorithm 4.2: FINDLINKPLUS(v_c, γ)

main
$link = \textbf{\textit{findLink}}(v_c)$
$adjacents = \textbf{\textit{findAdjacent}}(v_c, \gamma)$
$link.V = link.V - adjacents$
$stack = \emptyset$
for each $\textbf{\textit{presence}}(v_c, \gamma)$
do $v_0 =$ FINDPREDECESSOR($link.V$)
if $\delta(v_0) > \delta(v_c)$ **then** *break*
$stack = stack + v_0$
while not $(stack = \emptyset)$
do $intersections = \textbf{\textit{getLinkIntersections}}(v_0, v_c)$
for each $v_i \in intersections$
do **if** $(v_i \in link.V)$ **and not** $(v_i \in stack)$ **then** $stack = stack + v_i$
$link.V = link.V - v_0$
$stack = stack - v_0$
$v_0 = \textbf{\textit{next}}(stack)$
for each $v_a \in adjacents$
do $edge = \textbf{\textit{findEdgeConnecting}}(v_a, v_c)$
if $\textbf{\textit{presence}}(edge, \gamma) > 1$ **then** $adjacents = adjacents - (v_a)$
for each $edge \in link.E$
do **if not** $((edge.start$ **or** $edge.end) \in link.V)$ **or not** $((edge.start$ **or** $edge.end) \in adjacents)$ **then** $link.E = link.E - edge$
return $(\textbf{\textit{new}}(\gamma(link)))$

procedure FINDPREDECESSOR($link$)
$predecessor = \emptyset, d = \infty$
for each $v \in link$
do **if** $\delta(v) < d$ **then** $d = \delta(v)$; $predecessor = v$
return $(predecessor)$

4.2.5 Contour Split

The first condition to be checked for in order to detect split events is the multiple presence of v_c in the active contour (see Figure 10). Only when this condition occurs the entire active contour is explored, in order to isolate the connected sub-components.

When dealing in particular with coarse meshes with high genus, split and merge events can occur with high frequency and, omitting details, the resulting segments could be either fragmented or not simply connected. For this reason, after having detected a split event, it is important to determine which segment each contour vertex will belong after the split. In our method, after a split event, each of the two new segments will contain a connected subset of the splitting contour; this same connected subset is deemed

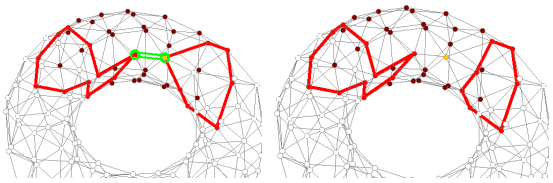

(a) (b)

Figure 10: Split event: the candidate vertex v_c (in orange) has a double presence in the active contour (a); the contour is split into two distinct ones (b).

the *originating vertices* of the segment. As a matter of fact, it can happen that the active contour γ that is splitting could contain one or more vertices belongings to the *originating vertices* of its own segment σ. If those vertices were simply passed to the two new segments, interruptions could be generated and the connectedness of the previous segment could be compromised. For this reason we introduce the idea of *multiple vertex membership*: vertices belonging to the *originating vertices* of a segment, if passed to other segments, will be marked as belongings to all involved segments. Figure 11 shows an example of *multiple vertex membership*: vertices with multiple membership are highlighted with a different border color. Inside vertex color represents parent segment belonging, border color represents child segment belonging. Higher level of sharing (e.g. vertices shared between three or more segments) can occur in practise for coarse meshes with higher genus.

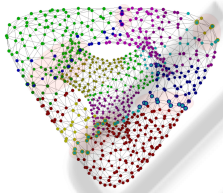

Figure 11: Vertices with multiple membership are in the highlighted areas in red.

4.2.6 Merge Between Contours

In analogy of the case of the split, the fundamental condition to be checked for in order to detect the occurrence of the merge event is the simultaneous presence of v_c in two contours (see Figure 12). When this is true, the two merging segments σ_1 and σ_2 are closed and stored in Σ_c and a new segment σ_{merged} is created. The merged active contour will also represent the *originating vertices* for the segment σ_{merged}.

4.2.7 Removing Folds

One of the real plagues of Morse functions, discretized in the way here described, is the presence

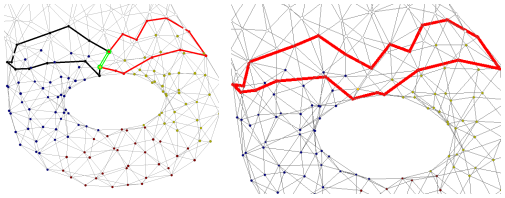

(a) (b)

Figure 12: Merge event: the candidate vertex v_c (in orange) belongs to two distinct contours (a); the two distinct contours are merged into one (b).

of multiple, spurious, local saddles, as analyzed in (Tierny et al., 2006). The algorithm could originate *false splits* when encountering those spurious saddles (see Figure 13). Indeed, in those cases, if we actually made a split, we would produce "anomalous contours", composed only by individual isolated vertices or contours where every edge would have a presence greater than one. We named situations like the one described in Figure 13 as *contour folds* and in our algorithm they are removed as soon as they occurs. Although we do not have a theoretical proof of the completeness of this solution, we tested it extensively and in our experimental evidence it solved the problem of spurious saddles completely. As shown in Figure 14 the check for fold presence can be performed once again in the basic step of active contour evolution: a fold is certainly present whenever a vertex with a single presence is connected with an edge with double presence. The fold-removing procedure is recursive in that it follows the fold "branch" until the latter is removed completely from the active contour. Obviously, the topology of the contour is unaffected by the fold-removing procedure.

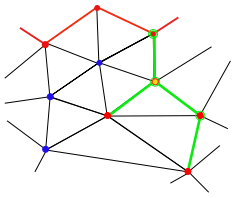

Figure 13: The candidate vertex v_c (in orange) is a spurious saddle.

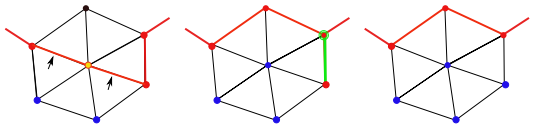

(a) (b) (c)

Figure 14: Removing folds: candidate v_c (in orange) is selected (a); a fold has been generated (in green) (b); the fold has been removed: the topology of the contour is unaffected (c).

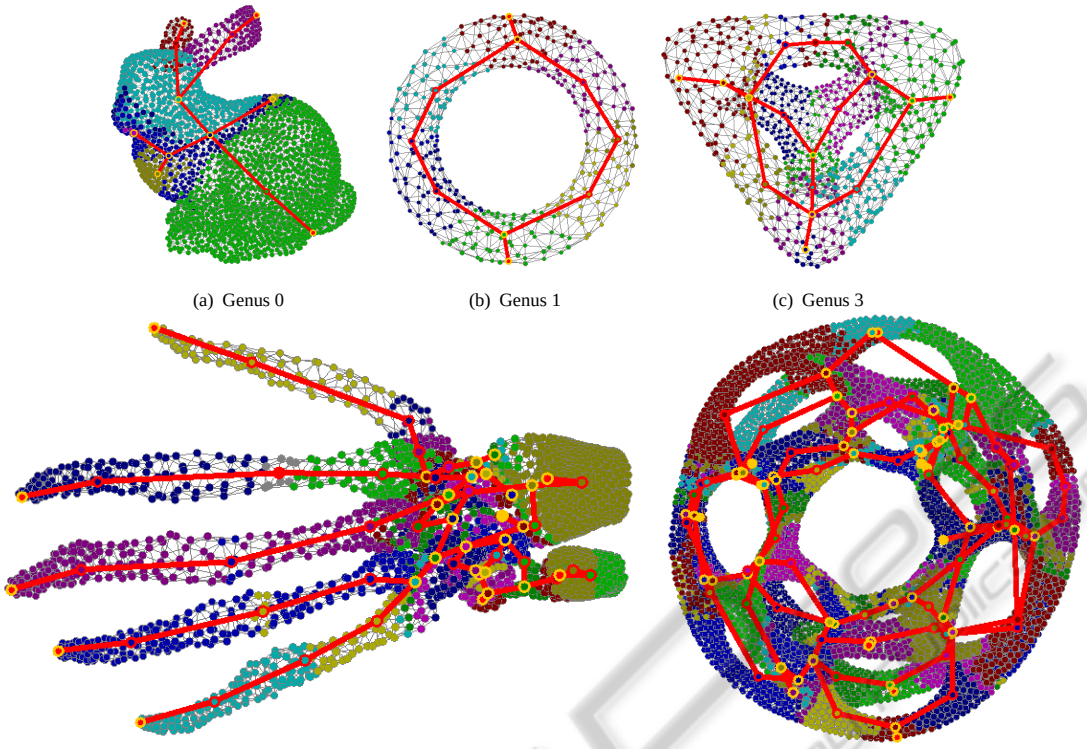

(a) Genus 0 (b) Genus 1 (c) Genus 3

(d) Genus 5 (e) Genus 22

Figure 16: A few meshes in the test set: Reeb graphs are painted in red, segmentations are highlighted with different vertices colors. Multiple vertex memberships are not represented in these images.

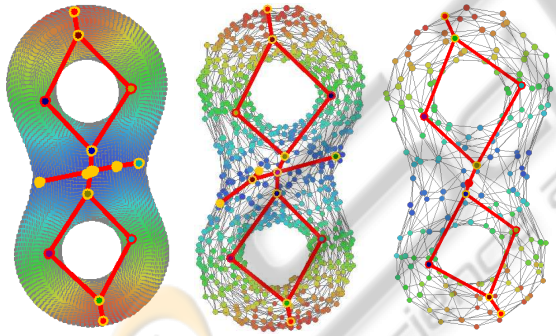

(a) (b) (c)

Figure 15: The original, high-resolution mesh with 12286 vertices (a), two increasingly decimated versions with random noise added, with 766 vertices (b) and 190 vertices (c).

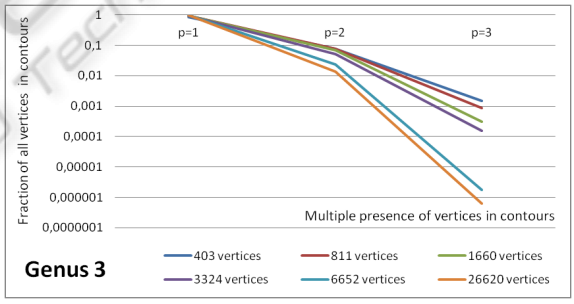

Figure 17: Progressive coarsening of the same mesh (Genus 3): a smaller number of vertices causes an increase of *multiple presences* in contours.

4.2.8 Constructing the Reeb Graph

In the output of our algorithm, each segment σ is a node in the Reeb graph and each arc corresponds to an adjacency relation between two segments, as described in Algorithm 4.1. The Reeb graph is built during active contour evolution. Every time an event occurs (either merge or split) and segments are stored in Σ_c, adjacency relations are also updated accordingly: after a merge the two merging segments are declared adjacent to the newly generated one; after a split the parent segment is declared adjacent to the two new ones.

5 EXPERIMENTAL EVIDENCE

In order to verify the correctness and effectiveness of the proposed algorithm we carried out extensive tests with a great number of meshes having different genus and density. We present here some of the most relevant results in our tests. Most of the meshes have

been taken from the AIM@Shape database (Falcidieno, 2004) and range from genus 0, both with great and small number of vertices, to genus 22 with over ten thousand vertices.

We used a non-optimized Java implementation because, at present, our main interest is the validation of the algorithm.

Since the algorithm contains a random choice of the starting point (see 4.1.1), our tests were carried out in an exhaustive way even with respect to the calculation of the diameter vertices. As a matter of fact, in order to test all the variants of the Morse function, we carried out, for each mesh, n test runs (with n being the number of mesh vertices), selecting at every run a different starting point, until every mesh vertex has been selected.

In order to validate the properties of the Reeb graphs obtained, we used the procedure described in (Safar et al., 2009) to compute the *minimum cycle basis* and hence the number of loops in each of those graphs. The number of loops must be equal to the genus of the corresponding mesh, which can be computed with the well-known Euler equation:

$$v - e + t = 2 - 2g \tag{2}$$

where v is the number of vertices in the mesh, e is the number of edges and t is the number of triangles.

With all the variants of the Morse function and for each of the meshes shown in Table 1, the proposed algorithm computes the Reeb graph corresponding to the correct genus. The meshes in the test set are also illustrated in Figure 16, together with the Reeb graphs and the segmentations obtained.

Finally, Figure 17(a) shows how coarser meshes lead to more complex active contours. The same mesh shown in Figure 16(c) has been considered at first with high resolution and then progressively decimated: in the statistics of these experiments multiple presences increase by orders of magnitude as the number of vertices decreases.

Table 1: Some of the meshes used to check the validity of the algorithm, with their genus and number of vertices.

Mesh Name	Genus	Vertices
Bunny	0	3052
Torus	1	359
Double torus-12286	2	12286
Double torus-766	2	766
Double torus-190	2	190
Genus3	3	782
HandG5	5	4037
HandG8	8	3639
Eptoroid	22	10851

6 CONCLUSIONS

As we have seen, the key aspect in the algorithm presented is the way in which active contours are evolved. Using the properties of the Morse function and the discrete topology of the triangle mesh, the evolution process can be performed by relying almost entirely on information being local to the vertices in the contours and their immediate neighborhood. In particular, it is not even necessary to verify at each step the connectedness of each active contour, because both split and merge events can only occur when the candidate vertex has multiple presence on one or more contours. A more complex test on the entire contour is only required when dealing with a split event, since the multiple presence of vertices and edges can make it more difficult to detect the connected components after the split.

Even if the theoretical validation of the correctness of the algorithm remains to be assessed, the experimental evidence presented supports the idea that the algorithm proposed could be effective for a wide class of real-world meshes.

ACKNOWLEDGEMENTS

The authors want to thank an anonymous reviewer for the precious comments and suggestions received.

REFERENCES

Berretti, S., Del Bimbo, A., and Pala, P. (2009). 3d mesh decomposition using reeb graphs. *Image and Vision Computing*, 27(10):1540 – 1554. Special Section: Computer Vision Methods for Ambient Intelligence.

Biasotti, S., Giorgi, D., Spagnuolo, M., and Falcidieno, B. (2008). Reeb graphs for shape analysis and applications. *Theoretical computer science*, 392:5–22.

Biasotti, S., Mortara, M., and Spagnuolo, M. (2000). Surface compression and reconstruction using reeb graphs and shape analysis. In *Proceedings of 16th Spring Conference on Computer Graphics*, pages 175–184. ACM press.

Cole-McLaughlin, K., Edelsbrunner, H., Harer, J., Natarajan, V., and Pascucci, V. (2003). Loops in reeb graphs of 2-manifolds. In *Proceedings of the nineteenth annual symposium on Computational geometry*, SCG '03, pages 344–350, New York, NY, USA. ACM.

Dijkstra, E. W. (1959). A note on two problems in connexion with graphs. *Numerische Mathematik*, 1:269271.

Doraiswamy, H. and Natarajan, V. (2009). Efficient algorithms for computing reeb graphs. *Computational Geometry*, 42(6-7):606 – 616.

Edelsbrunner, H. (2001). *Geometry and Topology for Mesh Generation*. Cambridge University Press, New York, NY, USA.

Edelsbrunner, H., Harer, J., Mascarenhas, A., Pascucci, V., and Snoeyink, J. (2008). Time-varying reeb graphs for continuous space-time data. *Computational Geometry*, 41(3):149 – 166.

Edelsbrunner, H., Harer, J., and Zomorodian, A. (2003). Hierarchical morse-smale complexes for piecewise linear 2-manifolds. *Discrete and Computational Geometry*, 30(1):87–107.

Falcidieno, B. (2004). Aim@shape project presentation. In *Shape Modeling Applications, 2004. Proceedings*, page 329.

Hilaga, M., Shinagawa, Y., Kohmura, T., and Kunii, T. L. (2001). Topology matching for fully automatic similarity estimation of 3d shapes. In *Proceedings of the 28th annual conference on Computer graphics and interactive techniques*, SIGGRAPH '01, pages 203–212, New York, NY, USA. ACM.

Katz, S., Leifman, G., and Tal, A. (2005). Mesh segmentation using feature point and core extraction. *The Visual Computer*, 21:649–658. 10.1007/s00371-005-0344-9.

Knuth, D. E. (1998). *The Art of Computer Programming Vol. 2: Seminumerical Algorithms*. Addison Wesley, 3rd edition.

Lazarus, F. and Verroust, A. (1999). Level set diagrams of polyhedral objects. In *Fifth Symposium on Solid Modeling*, pages 130–140. ACM.

Milnor, J. (1963). *Morse Theory*. Princeton University Press.

Mortara, M. and Patane, G. (2002). Affine-invariant skeleton of 3d shapes. *Shape Modeling and Applications, International Conference on*, 0:245–252.

Novotni, M., Klein, R., and Ii, I. F. I. (2002). Computing geodesic distances on triangular meshes. In *In Proc. of WSCG2002*, pages 341–347.

Pascucci, V., Scorzelli, G., Bremer, P.-T., and Mascarenhas, A. (2007). Robust on-line computation of reeb graphs: simplicity and speed. *ACM Trans. Graph.*, 26.

Patane, G., Spagnuolo, M., and Falcidieno, B. (2009). A minimal contouring approach to the computation of the reeb graph. *IEEE Transactions on Visualization and Computer Graphics*, 15:583–595.

Reeb, G. (1946). Sur les points singuliers d une forme de pfaff completement integrable ou d une fonction numerique. In *Comptes rendus de l'Academie des Sciences 222*, pages 847–849.

Safar, M., Alenzi, K., and Albehairy, S. (2009). Counting cycles in an undirected graph using dfs-xor algorithm. In *Networked Digital Technologies, 2009. NDT '09. First International Conference on*, pages 132 –139.

Schaefer, S. and Yuksel, C. (2007). Example-based skeleton extraction. In *Proceedings of the fifth Eurographics symposium on Geometry processing*, pages 153–162, Aire-la-Ville, Switzerland. Eurographics Association.

Sebastian, T., Klein, P., and Kimia, B. (2002). Shock-based indexing into large shape databases. In *Computer Vision ECCV 2002*, volume 2352 of *Lecture Notes in Computer Science*, pages 83–98. Springer Berlin / Heidelberg.

Shapira, L., Shamir, A., and Cohen-Or, D. (2008). Consistent mesh partitioning and skeletonization using the shape diameter function. *Visual Comput*, 24:249–259.

Shinagawa, Y. and Kunii, T. (1991). Constructing a reeb graph automatically from cross sections. *Computer Graphics and Applications, IEEE*, 11(6):44 –51.

Shinagawa, Y., Kunii, T., and Kergosien, Y. (1991). Surface coding based on morse theory. *Computer Graphics and Applications, IEEE*, 11(5):66 –78.

Sundar, H., Silver, D., Gagvani, N., and Dickinson, S. (2003). Skeleton based shape matching and retrieval. In *Shape Modeling International, 2003*, pages 130 – 139.

Tierny, J., Vandeborre, J., and Daoudi, M. (2006). 3d mesh skeleton extraction using topological and geometrical analyses. In *14th Pacific Conference on Computer Graphics and Applications*. Pacific Graphics.